Chemical Science International Journal
17(3): 1-14, 2016; Article no.CSIJ.29616
Previously known as American Chemical Science Journal
ISSN: 2249-0205

SCIENCEDOMAIN *international*
www.sciencedomain.org

Catalytic Conversion of Chloromethane to Methane and Propane on SiO_2/Al_2O_3: Kinetics of Deactivation Caused by Coking

Leopoldo O. A. Rojas[1*], João F. Sousa[2], Juan A. C. Ruiz[3] and Márcio B. D. Bezerra[2]

[1]Universidade Federal da Paraíba, UFPB/João Pessoa, Brazil.
[2]Universidade Federal do Rio Grande do Norte, UFRN/Natal, Brazil.
[3]Centro de Tecnologias do Gás e Energias Renováveis,CTGAS-ER/Natal, Brazil.

Authors' contributions

This work was carried out in collaboration between all authors. Author LOAR designed the study, synthetized and tested the catalysts. Author JFS analyzed results and edited the first draft of the manuscript. Author JACR helped with catalyst characterization and deactivation. Author MBDB managed literature searches and final editing. All authors read and approved the final manuscript.

Article Information

DOI: 10.9734/CSIJ/2016/29616
Editor(s):
(1) Georgiy B. Shul'pin, Semenov Institute of Chemical Physics, Russian Academy of Sciences, Moscow, Russia.
Reviewers:
(1) Vedrine Jacques, Universite P & M. Curie, Paris, France.
(2) Qingzhu Zhang, Shandong University, China.
(3) Sonia Bocanegra, Universidad Nacional del Litoral, Argentine.
Complete Peer review History: http://www.sciencedomain.org/review-history/16989

Original Research Article

Received 20th September 2016
Accepted 16th November 2016
Published 22nd November 2016

ABSTRACT

Chloromethane was catalytically converted into methane and propane in a fixed-bed reactor with control of pressure and flow rates. The deactivation by coking was studied in a microadsorber equipped with gravimetric monitoring. In this study, two models are proposed: the first one proposes that product production competes with coke formation; and the other one proposes that coke formation competes with product desorption. Kinetic and thermodynamic parameters were estimated. Results showed that chloromethane is activated by silica-alumina but the products are usually high molecular weight hydrocarbons, which are broken down by acid sites to produce compounds like methane and propane.

Keywords: Chloromethane; silica-alumina; deactivation; fixed-bed reactor; hydrocarbons.

**Corresponding author: E-mail: leopoldo@ct.ufpb.br;*
Co-author: E-mail: marciobarbalho@live.com;

1. INTRODUCTION

Methane conversion to higher hydrocarbons became one of the most important topics of natural gas utilization. Direct oxidation and oxidative coupling of methane with oxygen and other oxidants to higher hydrocarbons are extensively studied [1-5]. Due to its molecular stability, the functionalization and activation of the C–H bond is a difficult task [6,7]. On the other hand, halogenation of methane is a well-known reaction that usually requires the use of a catalyst [8,9]. The production of chloromethane through natural gas oxychlorination is an exothermic process that can be performed at low pressure and temperature. Under certain conditions, chloromethane can be converted into valuable hydrocarbons [8-10]. Hydrochloric acid is released in this second step and recycled to the first process. Thus, this constitutes an alternative route to the Fischer-Tropsch synthesis, as its operating conditions are much less stringent.

The conversion of chloromethane to hydrocarbons is heterolytic, where the chlorine is the highly electrophilic element [11,12]. After adsorption and splitting of chloromethane on the acid site, the chlorine will be adsorbed and a methyl group will be released. Methyl groups react via dehydrogenation to form a new group on the surface (preferably metallic) [10,13]. Hydrogen is released and transported across the surface (spillover) to find the adsorbed chlorine and form hydrochloric acid, which will eventually be desorbed. This mechanism is presented in Fig. 1. The species within the circle represents the catalytic surface and the adsorbed species therein. The gaseous species are adsorbed and desorbed according to the outer circle. The movement of hydrogen is depicted in the inner circle.

It is observed that there are two mechanisms that must operate in parallel, one on acidic sites, and the other one on metal sites. The catalysts on which these reactions take place are known to be bifunctional [13-15]. Their acidic function allows both the adsorption and the removal of chlorine from chloromethane while their metallic function promotes methyl groups condensation via dehydrogenation.

A major problem with the use of solid catalysts is the loss of activity (common factors are poisoning, coking or blocking and sintering or phase transformation) they exhibit over time. It is a physical and chemical process (usually inevitable), but there are techniques that can minimize the deactivation caused by these factors.

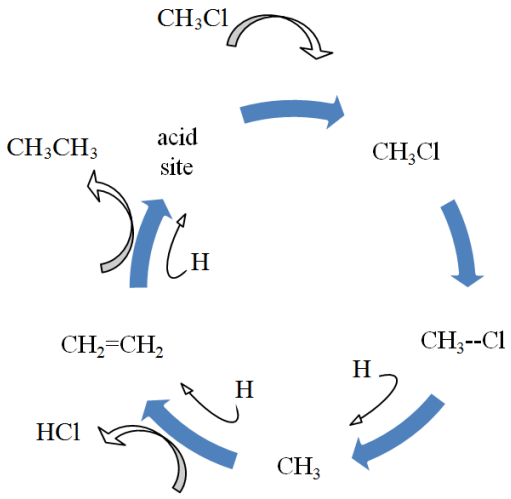

Fig. 1. CH_3Cl activation mechanism by Olah & Arpar [14]

Poisoning is a chemical process in which certain feed impurities are easily adsorbed on the catalyst active sites. The adsorption of a base on acid sites is an instance of poisoning. It can also be either a geometric process where the adsorbate covers the site or an electric effect where an electric field distorts the affinity adsorption of other adsorbates. Poisons may even chemically react with the site to form new products (reconstruction) such that the catalyst performance decreases.

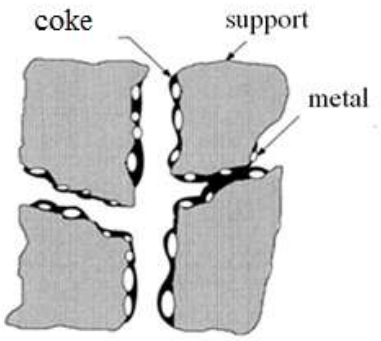

Fig. 2. Supported metal catalyst deactivation process: Encapsulation and pore blockage [16]

The chemical nature of coke depends on factors such as formation mechanism, pressure, temperature, feed composition, and products

formed. A representation of coke deposition is shown in Fig. 2. The catalyst deactivation may occur on mono or multi-layers of the sites and can completely encapsulate the metal, deactivating it. Other mechanisms include pore blockage, which prevents access of reagents to the active sites, carbon deposition, and growth within the pore, causing particle breakage.

In the case of coke formation from hydrocarbons, as in steam reforming, three types of carbon can be identified:

- C_nH_z: filamentous coke formed by slow polymerization over Ni at temperatures below 773 K;
- Filamentous char, also called whisker, formed by carbon diffusion in Ni followed by separation of Ni from the surface;
- Pyrolytic char from high molecular weight compounds cracking at temperatures above 873 K.

Sintering is a process where the catalyst is modified, mainly due to the effect of temperature. This process applies to both supported and massic catalysts. In the case of supported catalysts, the particles coalesce. One plausible explanation involves the separation of the metal from the crystallite and migration to another one with greater interaction field. As a result, large crystallites become larger while small crystallites become smaller.

The quantification of deactivation is very important, especially for processes with rapid loss of catalyst activity.

2. METHODS

2.1 Catalyst Testing

The catalytic activity tests were conducted using the experimental device shown in Fig. 3. The device consists of a gas supply system (1, 2 and 3), a mixture of CH_3Cl (10%) + N_2 (90%) and H_2 (99.99%), cylinder pressure regulators (4), mass flow controllers (5), a thermocouple (6), a furnace (7), a fixed-bed reactor (8), a gas purification system (9), a chromatograph (10) and a computer (11). The chlorine-resistant (hastelloy) reactor consists of a 50 cm tube with outer and inner dimeters of 1.27 cm and 0.635 cm, respectively. A stainless steel disc was placed inside the reactor to hold the catalytic bed in place.

2.2 Catalyst Deactivation

Catalytic tests were performed at the temperature of 573 K with unmodified and pure silica-alumina. The composition of the exhaust gases and the mass of deposited carbon (coke) were monitored simultaneously. The temperature of 573 K was chosen because, as reported by Comelli & Figoli [17] and Arevalo-Bastante et al. [18], it is the temperature at which coke formation starts. The equipment used for the evaluation was a Rubotherm microadsorber (Fig. 4) that consists of a basket in which the catalyst is placed. The basket is placed inside a vessel designed to support pressure up to 5 MPa and is suspended by a magnetic system without contact with the gases. Any variation in mass is compensated by a change in magnetic field intensity and recorded.

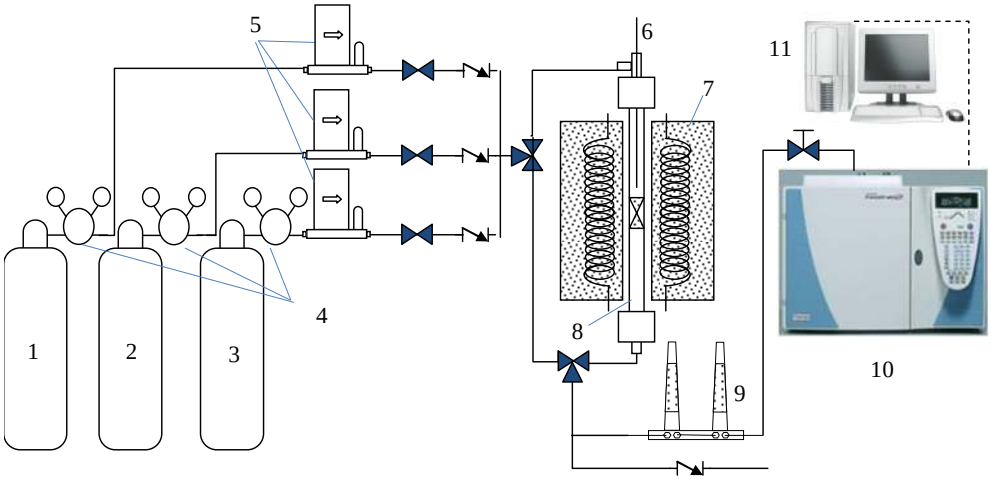

Fig. 3. Experimental apparatus used to evaluate the silica-alumina

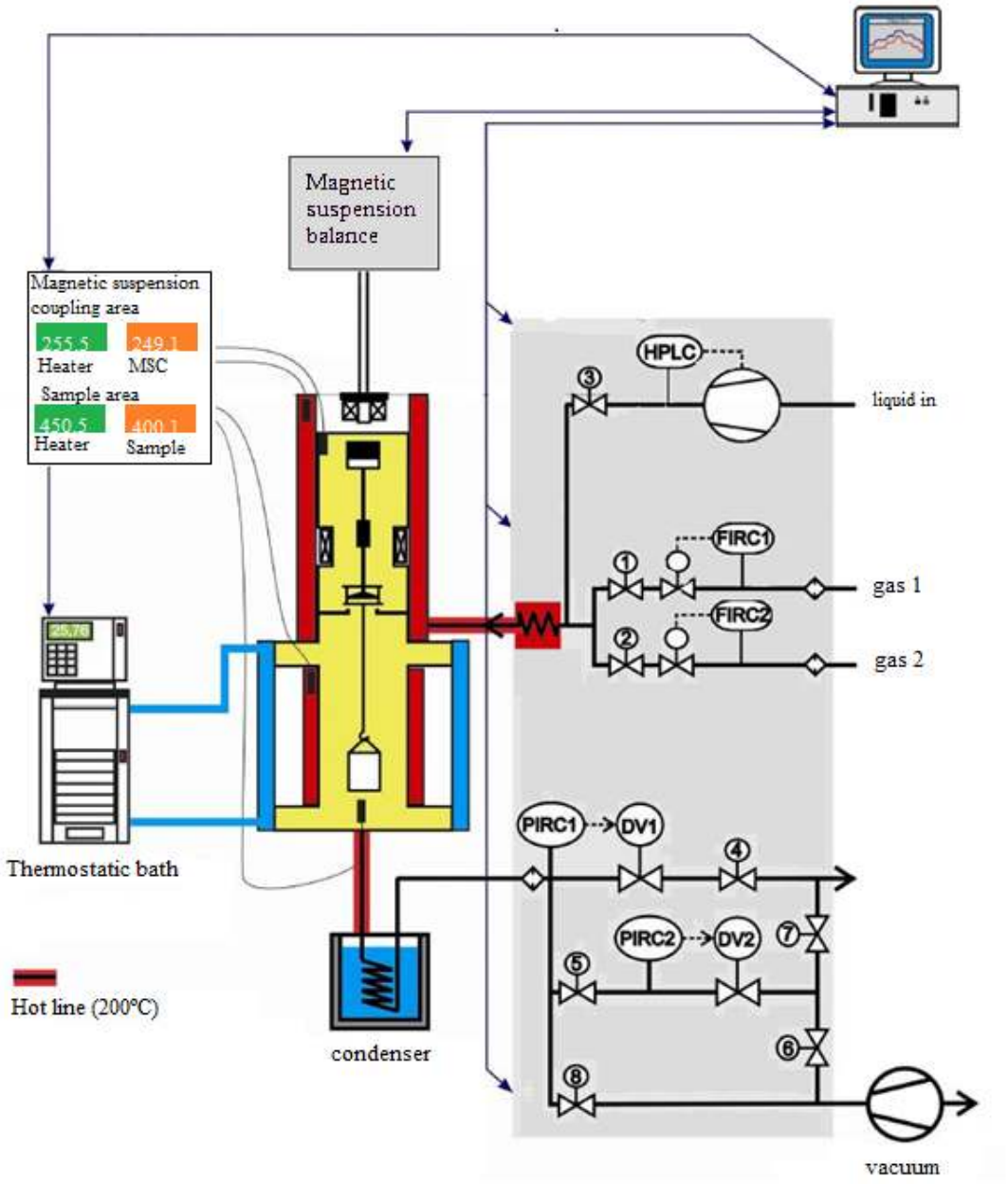

Fig. 4. Reaction system equipped with gravimetric monitoring. Adapted from Rojas [19]

The basket was loaded with approximately 250 mg of SiAl. After closing the reactor, the system was purged with helium 99.999% at a flow rate of 100 mL×min^{-1}. The material was then heated to 373 K for 30 minutes to avoid water adsorption. Afterwards, the reactor was heated to 573 K at a heating rate of 10 K×min^{-1}. After the system reached such temperature, the helium flow rate was reduced to 50 mL×min^{-1} and chloromethane was injected at the same rate. The reactions lasted 180 minutes with continuous monitoring of the catalyst mass. The outlet stream composition was determined using a Thermo C2V-200 3-channel micro-chromatograph. Each analysis took 2.5 minutes and the product composition was monitored every 3 minutes.

3. RESULTS AND DISCUSSION

The textural properties of the silica-alumina (Sigma-Aldrich, 99%) were obtained via adsorption with N_2 following the B.E.T method in

a Micrometrics ASAP 2020. The surface area was 513 $m^2 \times g^{-1}$, the average pore volume was 0.78 $cm^3 \times g^{-1}$, and the average pore diameter was 61.4 $\times 10^{-10}$ m.

3.1 Hydrocarbons Selectivity

The selectivity (S_i) is defined as the amount of carbon found in the species '*i*' formed:

$$S_i = \frac{\vartheta_i y_i^{out}}{\frac{y_{N_2}^{out}}{y_{N_2}^{in}}\left(y_{CH_3Cl}^{in} - y_{CH_3Cl}^{out}\right)} \quad (1)$$

The molar composition is represented by *y*, ϑ_i is the number of carbon atoms in the species '*i*' while the superscripts *in* and *out* indicate inlet and outlet, respectively.

The conversion and selectivity calculated for the tests with the silica-alumina are shown in Fig. 5.

It is observed that at the beginning of the reaction, t = 0, (time when the steady state is reached) the chloromethane conversion is approximately 65% and there is practically no gaseous products were formed. It is believed that this is temperature at which the chloromethane was converted into coke. This behavior is consistent with the results obtained by other researchers [8,20-22]. An induction time was present in this study, showing that chloromethane was converted into methyl-benzene compounds exclusively.

The chloromethane conversion with silica-alumina at the temperature of 573 K was about 60% at 723 K, 70% at 773 K and 95% at 823 K. Methane was the only product identified at temperatures above 723 K. The reaction system is inherently deficient in hydrogen so that the methane formation requires a source of that component. The conversion of chloromethane into compounds with low H/C ratios could be a source of hydrogen. In this case, H/C = 3, but whenever chloromethane reacts, an atom of hydrogen is released in the form of HCl and the original molecule becomes $–CH_2$. Two atoms of hydrogen are necessary for methane formation. As the first step does not produce gases, it is possible to propose the formation of large compounds with low H/C ratios. Also, as the reaction takes place, the surface concentration of free hydrogen increases to reach a critical value so that it promotes not only the reaction with $–CH_2$ to produce methane, but also desorption, as shown in Fig. 5. Traces of propane were observed at 773 K. As reported by Wei et al. [23-25], nanostructured catalysts such as ZSM-5 or SAPO-34 phosphate silicate have acid sites that favor the production of high amounts of coke and high molecular weight compounds. Due to their three-dimensional structure and size constraints, these large molecules cannot leave the catalytic structure and are broken down by acid sites. This same mechanism could be used to explain the propane formation.

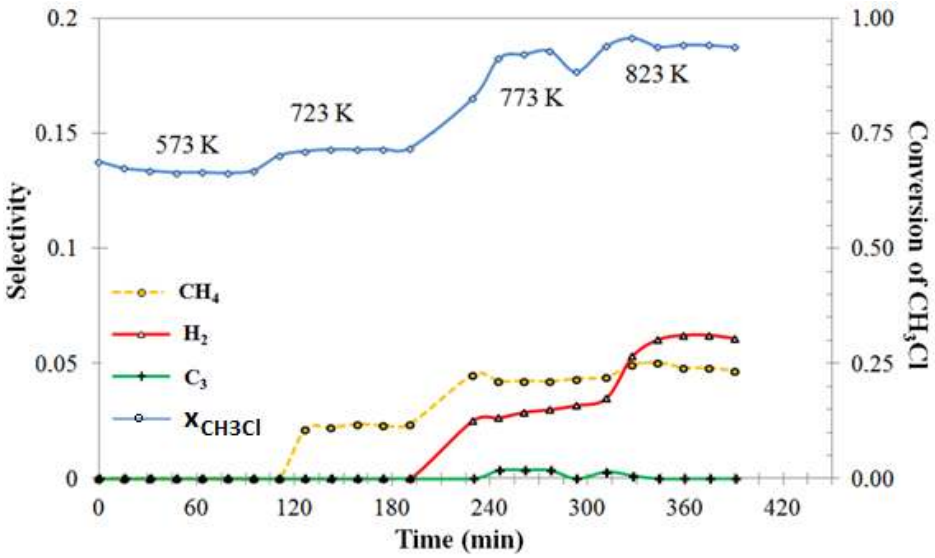

Fig. 5. Dynamic behavior of reactants and products on silica-alumina

The silica-alumina presented low selectivity for hydrocarbons. Even at high conversions, the products yields showed to be low at 573 K. Methane and hydrogen formation started at 723 K and 773 K, respectively. An increase in production of these compounds is an indication of high decomposition rates. The hydrogen production is indicative of compounds with low H/C ratios such as aromatics or free carbon. Since aromatic components were not identified, it is assumed that the product formed is free carbon.

3.2 Kinetic Mechanisms

Two reaction mechanisms are proposed in order to represent the chloromethane condensation deactivation. The first mechanism is described as parallel and the second is described as sequential (Fig. 6). Chloromethane is represented by **A**, hydrocarbons (methane and propane) are represented by **B,** and **C*** are the compounds that are formed and irreversibly adsorbed on the catalyst, also called coke. The term **B+1** refers to products release from the sites. For both mechanisms, **A** is adsorbed in the catalytic site that produces the constituent **B*** (adsorbed hydrocarbons), which desorbs to produce **B**.

For the parallel mechanism, coke (**C***) is formed from **A*** which competes with the formation of **B*** ($k_5 = k_{-5} = 0$), covering the catalyst surface. For sequential mechanism, coke is formed from **B*** ($k_4 = k_{-4} = 0$) and competes with its release from the catalytic site.

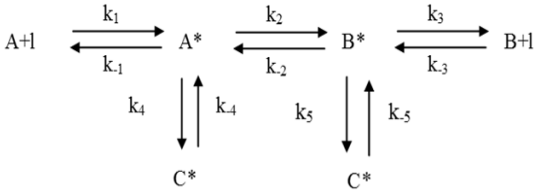

Fig. 6. Parallel and sequential mechanisms for coke formation. A = chloromethane, B = hydrocarbons, A* = B * = adsorbed hydrocarbons

The reaction rates and equilibrium constants used in this reaction system are shown in Table 1.

Assuming that the surface reaction is slow, it can be considered as the overall reaction. The chloromethane adsorption is represented by Eq. (12) and the product desorption by Eq. (13). Performing a balance on sites and considering the equilibrium equations mentioned in Table 1, an equation is obtained for site concentration. This process is summarized in Table 2.

Table 1. Elementary kinetic mechanisms and equilibrium constants

Mechanism	Kinetic model		Equilibrium constant	
A + l ⇌ (k1 / k-1) A*	$r_1 = k_1\left(C_A C_l\right) - k_{-1} C_{A^*}$	(2)	$K_A = \frac{C_{A^*}}{C_A C_l}$	(3)
A* ⇌ (k2 / k-2) B*	$r_2 = k_2 C_{A^*} - k_{-2} C_{B^*}$	(4)	$K_R = \frac{C_{B^*}}{C_{A^*}}$	(5)
B* ⇌ (k3 / -3) B + l	$r_3 = k_3\left(C_B^*\right) - k_3 C_B\ C_l$	(6)	$K_B = \frac{C_{B^*}}{C_B\ C_l}$	(7)
A* ⇌ (k4 / k-4) C*	$r_4 = k_4 C_{A^*} - k_{-4} C_{C^*}$	(8)	$K_C = \frac{C_{C^*}}{C_{A^*}}$	(9)
B* ⇌ (k5 / k-5) C*	$r_5 = k_5 C_{B^*} - k_{-5} C_{C^*}$	(10)	$K'_C = \frac{C_{C^*}}{C_{B^*}}$	(11)

where C_l is the free site concentration

Table 2. Site concentration descriptions

Expression		Description
$C_{A^*} = K_A C_A \; C_l$	(12)	adsorption of A
$C_{B^*} = K_B C_B \; C_l$	(13)	adsorption of B
$C_T = C_{A*} + C_{B*} + C_{C*} + C_l$	(14)	balance on sites
$C_l = \frac{C_T - C_{C*}}{1 + K_A C_A + K_B C_B}$	(15)	free site concentration - obtained substituting Eqs. (12) and (13) in (14)

3.2.1 Parallel mechanism

Combining Eqs. (4), (12), (13) and (14) we obtain Eq. (16):

$$r_2 = \frac{(C_T - C_{C*})}{C_T} \frac{k_2 K_A C_T \left(C_A - \frac{C_B}{K} \right)}{1 + K_A C_A + K_B C_B} \qquad (16)$$

where $K = K_r K_A / K_B$.

By definition, activity is the ratio between the reaction rate at an instant *t* and the initial reaction rate ($\varphi = r/r_0$). The activity can be obtained by dividing Eq. (16) by the initial rate (concentrations being constant):

$$\varphi_2 = \left(\frac{C_T - C_{C^*}}{C_T} \right)^{n_a} = \frac{r_2}{r_2^o} \qquad (17)$$

where n_a represents the sites involved in the reaction.

Combining Eqs. (16) and (17) yields:

$$r_2 = \phi_2 \frac{k_2 K_A C_T \left(C_A - \frac{C_B}{K} \right)}{1 + K_A C_A + K_B C_B} \qquad (18)$$

In order to derive an expression for coke formation rate, Eq. (8) should be taken into account in the parallel mechanism. As coke desorption is very slow, its constant is considered zero, $k_{-4} = 0$.

Combining Eqs. (8), (12), and (15) results in:

$$r_4 = \left[\frac{(C_T - C_{C^*})}{C_T} \right] \frac{k_4 K_A C_A C_T}{1 + K_A C_A + K_B C_B} \qquad (19)$$

The same approach given to the surface reaction, Eq. (17), can be extended to coke formation:

$$\varphi_C = \left(\frac{C_T - C_{C^*}}{C_T} \right)^{n_c} = \frac{r_C}{r_C^o} \qquad (20)$$

In general, n_c and n_a are not equal, and only will be if the number of sites required for both reactions are the same. Thus, substituting Eq. (20) in (19) leads to:

$$r_4 = \varphi_c^{\,n_c} \frac{k_4 K_A C_A C_T}{1 + K_A C_A + K_B C_B} \qquad (21)$$

3.2.2 Sequential mechanism

The coke formation can be given by Eq. (10) with $k_{-5} = 0$. Substituting Eq. (13) in Eq. (15), that expresses the number of free sites, yields:

$$r_5 = \left[\frac{(C_T - C_{C^*})}{C_T} \right] \frac{k_5 K_B C_B C_T}{1 + K_A C_A + K_B C_B} \qquad (22)$$

Using the definition of activity factor and combining Eqs. (20) and (22):

$$r_5 = \varphi_c^{\,n_c} \frac{k_5 K_B C_B C_T}{1 + K_A C_A + K_B C_B} \qquad (23)$$

Disregarding convective effects for a system of *Nr* reactions and *Nc* compounds, the mass balance for the compound *i* will be:

$$\frac{dC_i}{dt} = \sum_{j=1}^{N_r} \nu_{i,j} r_j \;, \forall\, i = 1, Nc \qquad (24)$$

where:

$\nu_{i,j}$ = stoichiometric coefficient of the compound *i* in reaction *j*;
r_j = conversion rate of reaction *j*.

Table 3 presents the balances of all components involved in the reactions studied.

The balance for the components **A**, **A***, **B**, **B***, **C*** considering the parallel mechanism are shown in Table 4 and those considering the sequential mechanism are presented in Table 5.

Table 3. Mass balance

(a) Parallel mechanism					
Reaction	**Compound**				
	A	**A***	**B***	**B**	**C***
2	0	$-r_2$	r_2	0	0
4	0	$-r_4$	0	0	r_4
$\Sigma v_{i,j} r_j$	0	$-r_2-r_4$	r_2	0	r_4
(b) Sequential mechanism					
Reaction	**Compound**				
	A	**A***	**B***	**B**	**C***
1	0	$-r_2$	r_2	0	0
5	0	0	$-r_5$	0	r_5
$\Sigma v_{i,j} r_j$	0	$-r_2$	$-r_2-r_5$	0	r_5

Table 4. Mass balance applied to coking using the parallel mechanism

I	**methane included**		**methane not included**	
A	$K_A = \frac{C_{A^*}}{C_A C_l}$	(25)	-	
A*	$\frac{dC_{A^*}}{dt} = -k_2 K_A C_L \left(C_A - \frac{C_B}{K} \right) - k_4 K_A C_A C_L$	(26)	$\frac{dC_A}{dt} = -\varphi_r \frac{k_2 K_A C_T \left(C_A - \frac{C_B}{K} \right)}{1 + K_A C_A + K_B C_B} - \varphi_c^{n_c} \frac{k_4 K_A C_A C_T}{1 + K_A C_A + K_B C_B}$	(27)
B*	$\frac{dC_B}{dt} = k_2 K_A C_l \left(C_A - \frac{C_B}{K} \right)$	(28)	$\frac{dC_{B^*}}{dt} = \varphi_r \frac{k_2 K_A C_T \left(C_A - \frac{C_B}{K} \right)}{1 + K_A C_A + K_B C_B}$	(29)
B	$K_B = \frac{C_{B^*}}{C_B C_l}$	(30)	-	
C*	$\frac{dC_c}{dt} = k_4 K_A C_A C_l$	(31)	$\frac{dC_{c^*}}{dt} = \varphi_c^{n_c} \frac{k_4 K_A C_A C_T}{1 + K_A C_A + K_B C_B}$	(32)

Table 5. Mass balance applied to coking using the sequential mechanism

I	**methane included**		**methane not included**	
A	$K_A = \frac{C_{A^*}}{C_A C_l}$	(33)	-	
A*	$\frac{dC_{A^*}}{dt} = -k_2 K_A C_l \left(C_A - \frac{C_B}{K} \right)_L$	(34)	$\frac{dC_{A^*}}{dt} = -\varphi_r \frac{k_2 K_A C_T \left(C_A - \frac{C_B}{K} \right)}{1 + K_A C_A + K_B C_B}$	(35)

I	methane included		methane not included	
B*	$\frac{dC_{B^*}}{dt} = k_2 K_A C_l \left(C_A - \frac{C_B}{K} \right) - k_5 K_B C_B C_l$	(36)	$\frac{dC_{B^*}}{dt} = \varphi_r \frac{k_2 K_A C_T \left(C_A - \frac{C_B}{K} \right)}{1 + K_A C_A + K_B C_B} - \varphi_c^{\,n_c} \frac{k_5 K_B C_B C_T}{1 + K_A C_A + K_B C_B}$	(37)
B	$K_B = \frac{C_{B^*}}{C_B \, C_l}$	(38)	-	
C*	$r_5 = k_5 K_B C_B C_l$	(39)	$r_5 = \varphi_c^{\,n_c} \frac{k_5 K_B C_B C_T}{1 + K_A C_A + K_B C_B}$	(40)

Given that **A** is in excess, it is assumed this constituent has constant concentration, so, substituting equilibrium relationships into reaction rates for this case, we get the following:

Species A*

$$\frac{dC_{A^*}}{dt} = K_A C_A \frac{dC_l}{dt} = -r_2 - r_4 = -k_2 K_A C_L \left(C_A - \frac{C_B}{K} \right) - k_4 K_A C_A C_L \tag{41}$$

From Eq. (41), it is possible to derive an equation for the catalyst free sites decrease.

Species B*

$$\begin{aligned} &\frac{dC_{B^*}}{dt} = K_B C_l \frac{dC_B}{dt} + K_B C_B \frac{dC_l}{dt} = K_B C_l \frac{dC_B}{dt} - \frac{K_B C_B}{K_A C_A} \left(r_2 + r_4 \right) = r_2 \\ &K_B C_l \frac{dC_B}{dt} = \left(\frac{K_B C_B}{K_A C_A} + 1 \right) r_2 + \frac{K_B C_B}{K_A C_A} r_4 \\ &\frac{dC_B}{dt} = \left(\frac{K_B C_B}{K_A C_A} + 1 \right) k_2 \frac{K_A}{K_B} \left(C_A - \frac{C_B}{K} \right) + C_B k_4 \end{aligned} \tag{42}$$

Rearranging Eq. (42):

$$\frac{d}{dt}\left(\frac{C_B}{C_A} \right) = -\frac{k_2}{K} \left(\left(\frac{C_B}{C_A} + \frac{K_A}{K_B} \right) \left(\frac{C_B}{C_A} - K \right) - \frac{C_B}{C_A} K \frac{k_4}{k_2} \right) \tag{43}$$

$$\frac{d}{dt}\left(\frac{C_B}{C_A} \right) = -\frac{k_2}{K} \left(\left(\frac{C_B}{C_A} \right)^2 - \left(-\frac{K_A}{K_B} + K + K \frac{k_4}{k_2} \right) \frac{C_B}{C_A} + \frac{K_A}{K_B} K \right) \tag{44}$$

By making $y = \frac{C_B}{C_A}$, the following expression is obtained:

$$\begin{aligned} &\frac{dy}{dt} = -\frac{k_2}{K} \left(y^2 - \left(-\frac{K_A}{K_B} + K + K \frac{k_4}{k_2} \right) y + \frac{K_A}{K_B} K \right) \\ &\frac{dy}{dt} = -a_3 \left(y - a_1 \right) \left(y - a_2 \right) \end{aligned} \tag{45}$$

where a_1 and a_2 are the roots of the second-order equation. These roots and the coefficient a_3 are related to the differential equation parameters by the following equations:

$$(a) \qquad a_1 + a_2 = \left(-\frac{K_A}{K_B} + K + K\frac{k_4}{k_2} \right)$$

$$(b) \qquad a_1 a_2 = \left(\frac{K_A}{K_B} K \right) \tag{46}$$

$$(c) \qquad a_3 = -\frac{k_2}{K}$$

Solving the differential equation with $y(0)=y_0$:

$$\int_{y_o}^{y} \frac{dy}{(y-a_1)(y-a_2)} = \frac{-1}{a_1-a_2}\left(\int_{y_o}^{y} \frac{dy}{y-a_1} - \int_{y_o}^{y} \frac{dy}{y-a_2} \right) = \frac{-1}{a_1-a_2}\left[\ln\left(\frac{y-a_1}{y-a_2} \right) - \ln\left(\frac{y_o-a_1}{y_o-a_2} \right) \right] \tag{47}$$

$$\int_{y_o}^{y} \frac{dy}{(y-a_1)(y-a_2)} = \int_{t_o}^{t} -a_3\, dt \tag{48}$$

$$\ln\left(\frac{y-a_1}{y-a_2} \right) - \ln\left(\frac{y_o-a_1}{y_o-a_2} \right) = a_3(a_1-a_2)(t-t_o)$$
$$\frac{y-a_1}{y-a_2} = \left(\frac{y_o-a_1}{y_o-a_2} \right)\exp\left(a_3(a_1-a_2)(t-t_o) \right) \tag{49}$$

$$y = a_1 + (a_1-a_2)\frac{\left(\frac{y_o-a_1}{y_o-a_2} \right)\exp\left(a_3(a_1-a_2)t \right)}{1-\left(\frac{y_o-a_1}{y_o-a_2} \right)\exp\left(a_3(a_1-a_2)t \right)} \tag{50}$$

Rearranging and returning to the original variable, we obtain:

$$y = \frac{C_B}{C_A} = \frac{a_1 - a_2\left(\frac{y_o-a_1}{y_o-a_2} \right)\exp\left(a_3(a_1-a_2)t \right)}{1-\left(\frac{y_o-a_1}{y_o-a_2} \right)\exp\left(a_3(a_1-a_2)t \right)} \tag{51}$$

$$y_o = \frac{C_{Bo}}{C_{Ao}}$$

Thus, the profile of B, as seen in Eq. (51), is a function of the following parameters:

$C_B = g(t, \underline{a})$
a_i: parameter i, i=1, 2, 3

Species C*

$$\frac{dC_c}{dt} = \varphi_c^{\,n_c} \frac{k_4 K_A C_A C_T}{1 + K_A C_A + K_B C_B} \tag{52}$$

Substituting C_B from Eq. (51) in Eq. (52):

$$\frac{1}{\varphi^{nc}} \frac{d\varphi_c}{dt} = k_4 \frac{K_A C_A}{\left(1 + K_A C_A + K_B a_2\right)} \left[1 + \frac{K_B \left(a_2 - a_1\right)}{\left(1 + K_A C_A + K_B a_1\right) - \left[\left(1 + K_A C_A + K_B a_2\right) \left(\frac{y_o - a_1}{y_o - a_2} \right) \exp\left(a_3 \left(a_1 - a_2\right) t\right) \right]} \right] \tag{53}$$

Integrating Eq. (53) subjected to $y(0)=y_0$, we obtain:

$$\frac{\varphi^{1-nc} - 1}{1 - n_c} = -\frac{K k_4}{k_2} \frac{K_A C_A}{\left(1 + K_A C_A + K_B a_2\right)\left(1 + K_A C_A + K_B a_1\right)} \left[t\left(1 + K_A C_A + K_B a_1\right) + K_B \left(a_3 \left(a_1 - a_2\right) t\right) + K_B \log \left[\frac{\left(1 + K_A C_A + K_B a_1\right) - \left[\left(1 + K_A C_A + K_B a_2\right) \left(\frac{y_o - a_1}{y_o - a_2} \right) \exp\left(a_3 \left(a_1 - a_2\right) t\right) \right]}{\left(1 + K_A C_A + K_B a_1\right) - \left[\left(1 + K_A C_A + K_B a_2\right) \left(\frac{y_o - a_1}{y_o - a_2} \right) \right]} \right] \right] \tag{54}$$

C_A is known, so the parameters to be calculated are K_A, K_B and n_c. The activity is then a function of time and six parameters:

$\varphi = f(t, \underline{a})$
a_i: parameter i, i=1, 6

where the parameters a_1, a_2 and a_3 are inserted in Eq. (51) and the new parameters are:

$$\begin{aligned} a_4 &= K_A \\ a_5 &= K_B \\ a_6 &= n_c \end{aligned} \tag{55}$$

3.3 Parameter Estimation

The concentration discrete values, the support mass gain and the activity are presented as functions of time.

So we have two sets of points $\underline{\boldsymbol{P}}$ and $\underline{\boldsymbol{Q}}$ such that:

$$\begin{aligned} P_i &= \left(t_i, C_{B\_\exp,i}\right), \quad i = 1, n_P \\ Q_j &= \left(t_j, \varphi_{\_\exp,j}\right), \quad j = 1, n_Q \end{aligned} \tag{56}$$

The two-term objective function to be minimized is as follows:

$$FO = \min \left[\sum_{i=1}^{n_P} \left(C_{B\_\exp,i} - g(t_i, a_1, a_2, a_3)\right)^2 + \sum_{j=1}^{n_Q} \left(\varphi_{\_\exp,j} - f\left(t_j, \underline{a}\right)\right)^2 \right] \tag{57}$$

where the set of parameters (a) are adjusted to meet the minimum of the objective function. The data and their expressions of concentration and activity were tabulated in an excel spreadsheet. The sum of squared difference between the experimental and calculated values, Eq. (57), was minimized using Excel's SOLVER and the

nonlinear Generalized Reduced Gradient (GRG) method.

The deactivation kinetic parameters, from Eqs. (46) and (55), are shown in Table 6.

Table 6. Parameters estimated using the parallel mechanism

	Description	Value	Unit
K_A	Adsorption of A	0.0042	kPa^{-1}
K_B	Adsorption of B	0.0227	kPa^{-1}
K	Overall equilibrium constant	0.0030	
k_2	Kinetic Constant of reaction 2	8.01×10^{-4}	min^{-1}
k_4	Kinetic constant of coke formation	1.46×10^{-1}	min^{-1}
n_c	Activity exponent of coke	1.516	

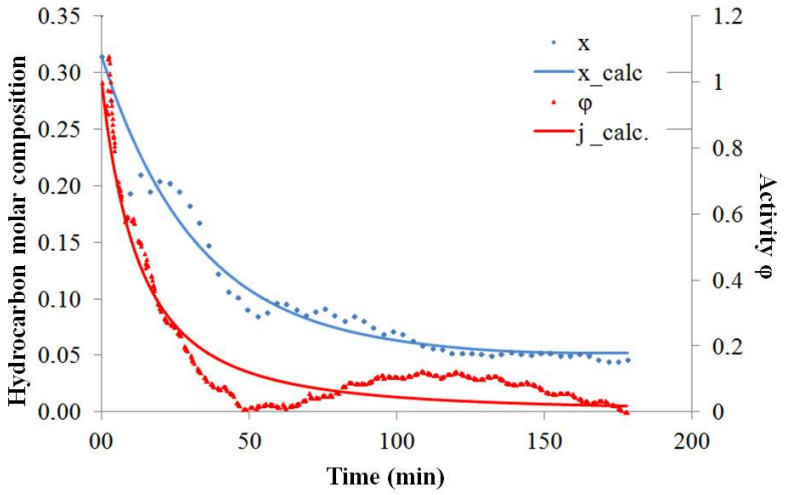

Fig. 7. Conversion of chloromethane on silica-alumina at 573 K – parallel mechanism

From the results shown in Table 6, it can be observed that the reactant adsorption constant (A = chloromethane, B = hydrocarbons) and the product desorption constant are 0.0042 kPa^{-1} and 0.0227 kPa^{-1}, respectively, indicating that the adsorption driving force of A is of the same magnitude order as that of desorption of B. The low value of the global constant (0.003) is in agreement with thermodynamics which states that the reaction is unfavorable for hydrocarbon formation. The reaction kinetic constant (8.01×10^{-4} min^{-1}) is a thousand times smaller than the kinetic constant related to coke formation (1.46×10^{-1} min^{-1}), which means that the reaction system under these operating conditions favors coke formation at the expense of hydrocarbon formation. The exponent of the activity of coke is 1.516, which means that this reaction is more demanding of sites than the hydrocarbon formation.

The parallel mechanism model was the only one whose equations fitted the data well. As presented in Fig. 7, the hydrocarbon molar composition decreases with time at a rate similar to that of the activity factor.

4. CONCLUSIONS

The silica-alumina activates the chloromethane, but without enough hydrogen, it promotes the formation of compounds with low H/C ratios and high molecular weight. These compounds are difficult to desorb and end up accumulating on the catalyst surface. An increase in hydrocarbon concentration increases the amount of free hydrogen which reacts to produce methane and hydrogen after release. The parameters obtained from the fit of the model confirmed the low reaction rate for hydrocarbon formation, justifying the consideration of choosing this reaction as limiting. The coke formation rate is a thousand times greater than the hydrocarbon formation rate; therefore coke formation is greater than hydrocarbon formation. The exponent of coke activity being higher than 1 (approx. 1.6)

indicates that the coke coating rate is greater than the reagent coating rate (A*). Thus, the parallel mechanism model is adequate to represent the deactivation over silica-alumina.

COMPETING INTERESTS

Authors have declared that no competing interests exist.

REFERENCES

1. We Comelli Y, Figoli I, Zhang D, Liu Z, Su BL. Mechanistic elucidation of chloromethane transformation over SAPO-34 using deuterated probe molecule: A FTIR study on the surface evolution of catalyst. Chemical Physics Letters. 2007;444(1-3):197-201.
2. Denis Jaumain, Bao-Lian Su. Direct catalytic conversion of chloromethane to higher hydrocarbons over a series of ZSM-5 zeolites exchanged with alkali cations. Journal of Molecular Catalysis A: Chemical. 2003;263-273.
3. Ling-tao Kong, Ben-xian Shen, Zhang Jiang, Ji-gang Zhao, Ji-chang Liu. Synthesis of SAPO-34 with the presence of additives and their catalytic performance in the transformation of chloromethane to olefins. Reac Kinet Mech Cat. 2015;697-710.
4. Dazhi Zhang, Yingxu, Lei Xu, Aiping Du, Fuxiang Chang, Bao-lian Su, Zhongmin Liu. Chloromethane conversion to higher hydrocarbons over zeolites and SAPOs. Catalysis Letters. 2006;97-101.
5. Martin-Martinez M, Gómez-Sainero LM, Alvarez-Montero MA, Bedia J, Rodriguez JJ. Comparison of different precious metals in activated carbon-supported catalysts for the gas-phase hydro-dechlorination of chloromethanes. Appl. Cat. B. Environ. 2013;131-132:256-265.
6. Sachchit Majhi, Pravakar Mohanty, Hui Wang, Pant KK. Direct conversion of natural gas to higher hydrocarbons: A review. Journal of Energy Chemistry. 2013;22:543-554.
7. Unni Olsbye, Ole Vaaland Saure, Naresh Babu Muddada, Silvia Bordiga, Carlo Lamberti, Merete Hellner Nilsen, Karl Petter Lillerud, Stian Svelle. Methane conversion to light olefins—How does the methyl halide route differ? Catalysis Today. 2011;171:211-220.
8. Ling-tao Kong, Ben-xian Shen, Ji-gang Zhao, Ji-chang Liu. Comparative study on the chloromethane to olefins reaction over SAPO-34 and HZSM-22. Industrial & Engineering Chemistry Research. 2014; 16324-16331.
9. Leandro A Noronha, Falabella Souza-Aguiar E, Claudio JA Mota. Conversion of chloromethane to light olefins catalyzed by ZSM-5 zeolites. Catalysis Today. 2005;9-13.
10. Merete Hellner Nilsen, Stian Svelle, Sharmala Aravinthan, Unni Olsbye. The conversion of chloromethane to light olefins over SAPO-34: The influence of dichloromethane addition. Applied Catalysis A: General. 2009;23-31.
11. Olah GA. USPAT. 1983;109(4):373.
12. Monica Gamero, Andres T Aguayo, Ainara Ateka, Paula Pérez-Uriarte, Ana G Gayubo, Javier Bilbao. Role of shape selectivity and catalyst acidity in the transformation of chloromethane into light olefins. Industrial & Engineering Research Chemistry. 2015;7822-7832.
13. Khaleel A, Shehadi I, Al-Marzouqi A. Catalytic conversion of chloromethane to methanol and dimethyl ether over mesoporous γ-alumina. Fuel Proc. Technol. 2011;92:1783-1789.
14. Olah GA, Arpadr A. Hydrocarbon chemistry. New Jersey: Wiley Inter Science; 2003.
15. Yingxu Wei, Dazhi Zhang, Zhongmin Liu, Bao-Lian Su. Methyl halide to olefins and gasoline over zeolites and SAPO catalysts: A new route of MTO and MTG. Chinese Journal of Catalysis. 2012;33(1):11-21.
16. Bartholomew HC. Mechanisms of catalyst deactivation. Applied Catalysis A: General. 2001;212:17-60.
17. Comelli R, Figoli N. Effect of pressure on the transformation of methanol into hydrocarbons on an amorphous silica-alumina. Applied Catalysis. 1991;73(2): 185-194.
18. Arevalo-Bastante A, Álvarez-Montero MA, Bedia J, Gómez-Sainero LM, Rodriguez JJ. Gas-phase hydrodechlorination of mixtures of chloromethanes with activated carbon-supported platinum catalysts. Appl. Cat. B: Environ. 2015;179:551-557.
19. Rojas LOA. Conversão catalítica de clorometano em hidrocarbonetos. (PhD Thesis) Programa de Pós-Graduação em Engenharia Química - (PPGEQ) - UFRN/Natal - Brazil; 2012.
20. Svelle S, Aravinthan S, Bjogen M, Lillerud KP, Kolboe S, Dahl IM. The methyl halide

to hydrocarbon reaction over H-SAPO-34. Journal of Catalysis. 2006;241(2):243-254.
21. Zhang D, Wei Y, Xu L, Du A, Chang F, Su B, Liu Z. Chloromethane conversion to higher hydrocarbons over zeolites and SAPOs. Catal. Lett. 2006;109:97-101.
22. Li N, Zhang Y, Chen L, Au C, Yin S. Synthesis and application of HZSM-5@silicalite-1 core-shell composites for the generation of light olefins from CH_3Br. Micropor. Mesopor. Mat. 2016;76-80.
23. Wei Y, Zhang D, Xu L, Liu Z, Su B. New route for light olefins reaction over SAPO-34 molecular sieve. Catal. Today. 2005;106:84-89.
24. Wei Y, Zhang D, Chang F, Xia Q, Su B, Liu Z. Ultra-short contact time conversion of chloromethane to olefins over pre-coked SAPO-34: Direct insight into the primary conversion with coke deposition. Chem. Commum. 2009;40:5999-6001.
25. Wei Y, Zhang D, liu Z, Su B. Methyl Halide to olefins and gasoline over zeolites and SAPO catalysts: A new route of MTO and MTG. Chin. J. Cat. 2012;33(1):11-21.

Peer-review history:
The peer review history for this paper can be accessed here:
http://sciencedomain.org/review-history/16989